RSC Advances

PAPER

View Article Online
View Journal | View Issue

Cite this: *RSC Adv.*, 2018, **8**, 28139

Asymmetric ring-opening reaction of *meso*-epoxides with aromatic amines using homochiral metal–organic frameworks as recyclable heterogeneous catalysts†

Koichi Tanaka, *[a] Maya Kinoshita,[a] Jun Kayahara,[a] Yutaro Uebayashi,[a] Kazusada Nakaji,[a] Maja Morawiak[b] and Zofia Urbanczyk-Lipkowska[b]

Received 16th June 2018
Accepted 31st July 2018

DOI: 10.1039/c8ra05163a

rsc.li/rsc-advances

An efficient asymmetric ring-opening (ARO) reaction of *meso*-epoxides with aromatic amines catalysed by a series of homochiral metal–organic frameworks (MOFs) was carried out. Excellent results (up to 95% ee) for the ARO of cyclohexene oxide with several aromatic amines were achieved with a homochiral MOF derived from the ligand (*R*)-2,2′-dihydroxyl-1,1′-binaphthalene-5,5′-dicarboxylic acid. Furthermore, homochiral MOFs based on (*R*)-2,2′-dihydroxy-1,1′-binaphthyl-4,4′-di(4-benzoic acid) and (*R*)-2,2′-diethoxy-1,1′-binaphthyl-4,4′-di(5-isophthalic acid) catalysed ARO reactions of *cis*-stilbene oxide with 1-naphthylamine in high yield (up to 95%) and excellent enantioselectivity (up to 97%) of the β-amino alcohol. The MOF catalysts were recoverable and recyclable with retention of their performance.

Introduction

Chiral β-amino alcohols are useful building blocks for biologically active natural products such as therapeutic agents, β-blockers, insecticidal agents, antimalarial agents and oxazolines,[1] as well as important auxiliaries and ligands in asymmetric synthesis.[2] Several methods for the asymmetric synthesis of these compounds have been developed. Among them, the catalytic asymmetric ring opening (ARO) of *meso*-epoxides with amines is one of the most important and straightforward strategies to synthesize optically enriched β-amino alcohols.[3] Several reports have appeared for the synthesis of β-amino alcohols through the ARO of *meso*-epoxides with anilines.[4] However, homogeneous catalysts have been widely applied. Porous metal–organic frameworks (MOFs) with high surface areas and thermal stabilities have attracted much attention recently owing to their versatile applications in storage,[5] separation,[6] sensing,[7] and catalysis.[8] In particular, chiral MOFs, which are assembled using chiral organic ligands and metal ions, are of interest for applications in enantioselective separation and catalysis, which are important for the pharmaceutical industry. In 2008, we reported the synthesis of (*R*)-CuMOF-**1**[9a] by treating (*R*)-2,2′-dihydroxyl-1,1′-binaphthalene-5,5′-dicarboxylic acid **1** with $Cu(NO_3)_2$, and investigated its catalytic activity toward ARO reactions of cyclohexene oxide with some aniline derivatives to furnish the corresponding β-amino alcohols in moderate enantioselectivities ranging from 43–51% ee.[9a] Recently, we synthesized (*R*)-CuMOF-**2** from (*R*)-2,2′-dihydroxyl-1,1′-binaphthalene-4,4′-di(4-benzoic acid) **2** and its application to the efficient heterogeneous catalyst for the asymmetric Diels–Alder reaction of isoprene with *N*-ethyl maleimide has been reported.[10] We also constracted (*R*)-CuMOF-**3** from (*R*)-2,2′-dihydroxyl-1,1′-binaphthalene-5,5′-di(4-benzoic acid) **3**, which exhibited high catalytic activity in the Diels–Alder reaction of acrolein and 1,3-cyclohexadiene.[11]

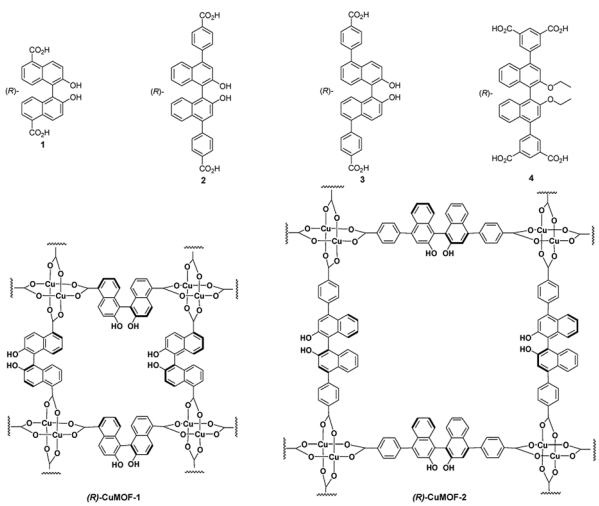

[a]*Department of Chemistry and Materials Engineering, Faculty of Chemistry, Materials and Bioengineering, Kansai University, Suita, Osaka 564-8680, Japan. E-mail: ktanaka@kansai-u.ac.jp; Fax: +81-06-6368-0861; Tel: +81-06-6368-0861*

[b]*Institute of Organic Chemistry, Polish Academy of Sciences, Kasprzaka 44/52, 01-224 Warszawa, Poland. E-mail: ocryst@icho.edu.pl; Fax: +48 22 6326681; Tel: +48 22 3432207*

† Electronic supplementary information (ESI) available: Details of synthesis of (*R*)-ZnMOF-**1**, catalytic asymmetric ring opening reactions, IR, TG, NMR spectra, HPLC chromatographic data. CCDC 1832085. For ESI and crystallographic data in CIF or other electronic format see DOI: 10.1039/c8ra05163a

In this study, we report the synthesis of a novel homochiral (*R*)-ZnMOF-**4** from (*R*)-2,2′-dihydroxy-1,1′-binaphthyl-4,4′-di(5-isophthalic acid) **4** and the application of (*R*)-CuMOF-**1**, (*R*)-CuMOF-**2**, (*R*)-CuMOF-**3** and (*R*)-ZnMOF-**4** as recyclable heterogeneous catalysts for the ARO reaction of *meso*-epoxides with some aromatic amines to form optically active β-amino alcohols.

Results and discussion

Synthesis of (*R*)-CuMOF-1, (*R*)-CuMOF-2 and (*R*)-CuMOF-3

(*R*)-CuMOF-**1**,[9] (*R*)-CuMOF-**2**[10] and (*R*)-CuMOF-**3**[11] were synthesized by the methods reported earlier.

Synthesis and characterization of a new (*R*)-ZnMOF-4

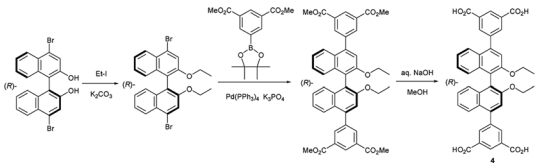

Chiral organic ligand (*R*)-2,2′-dihydroxy-1,1′-binaphthyl-4,4′-di(5-isophthalic acid) **4** was synthesized by Suzuki cross-coupling of dimethyl 5-(4,4,5,5-tetramethyl-1,3,2-dioxaborolan-2-yl)isophthalate and (*R*)-4,4′-dibromo-2,2′-diethoxy-1,1′-binaphthyl (prepared from (*R*)-4,4′-dibromo-2,2′-dihydroxy-1,1′-binaphthyl),[12] followed by hydrolysis and acidification. (*R*)-ZnMOF-**4** was obtained as pale-yellow prisms after a solvothermal reaction of the chiral organic linker (*R*)-**4** and $Zn(NO_3)_2 \cdot 6H_2O$ in a mixed solvent (*N*,*N*-dimethylacetamide–EtOH) at 110 °C for 2 days. The structure was characterized by IR spectroscopy (Fig. S1†), thermogravimetric analysis (Fig. S2†), solid CD spectroscopy (Fig. S3†). The observed powder XRD patterns (Fig. S4†) are the same as the simulated ones (Fig. S5†), demonstrating phase purity of the bulk samples. N_2 adsorption isotherm (Fig. S6†) and BET plot (Fig. S7†) of (*R*)-ZnMOF-**4** were also determined.

X-ray diffraction analysis revealed that a rigid metal–organic framework was constructed around two pentacoordinated Zn(II) cations with the nearest Zn1···Zn2 distance 3.384(2) Å, which were bridged by three carboxy groups from three different chiral ligands (Fig. 1). The Zn1–O distances were 1.977(4) Å–2.062(6) Å, and the Zn2–O lengths span was in the range of 1.940(5)–2.476(5) Å. A trigonal bipyramidal coordination sphere of Zn1 cation was completed by another monodentate carboxylate, one water and one C, whereas the coordination sphere of the Zn2 had as geometry of a very distorted trigonal bipyramid and was completed by one monodentate carboxy groups (Fig. S6†). Other structural features that may be essential for the catalytic process is the presence of three *N*,*N*-dimethylacetamide molecules in the structure – one coordinated to Zn1 and two trapped in the crystal lattice by a few C–H···O hydrogen bonds. The crystal contained two *N*,*N*-dimethylcetamide, one water and one ethanol molecules, all with half occupancy. A low *R*-factor (0.0664), reasonable goodness-of-fit (1.08) and small residual density (0.83 e) suggested that no additional solvent molecules

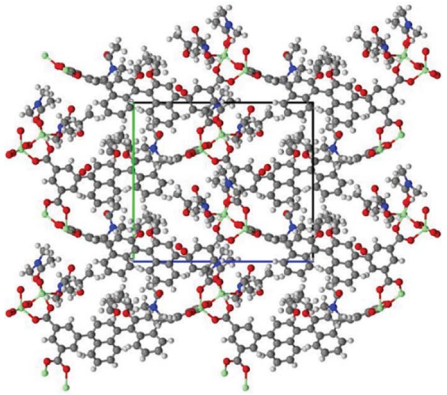

Fig. 1 X-ray structure of (*R*)-ZnMOF-**4**, shown down *a*-axis. Color codes: Zn(II) – green, O – red, N – blue, C, H – grey.

were present in crystals. A collection of separate voids present in the unit cell of (*R*)-ZnMOF-**4** occupies only *ca.* 275 $Å^3$ (8.6%) of the total unit cell volume (Fig. S7†).

When all solvent molecules excluding one scaffold-firming and coordinated to Zn(II) *N*,*N*-dimethylacetamide molecule were removed the structure became more porous. In such case, the calculated volume of Connolly's surface[13] that was accessible for substrates (solvent) adsorption–desorption process was enhanced to 1329 $Å^3$, *i.e.* 41% of the unit cell volume. The analysis of a spatial distribution of possible transportation pathways in the chiral (*R*)-ZnMOF-**4** revealed that there are two channels present in the crystals that are oriented along *a*-axis. Their estimated cross-sections are: for channel 1 – 4.7 × 7.7 Å and for channel 2 – 5.6 × 5.6 Å (Fig. 2 and S6†). It is obvious from these estimations that all solvated epoxides as well as aniline derivatives fit well to both channels. Moreover, both channels have large chiral side compartments where reaction might proceed and products might be temporarily stored. Molecular dimensions of the reaction product **8a** calculated from X-ray data (CCDC 281038)[14] suggest that such molecules might migrate down the channels, particularly when raising temperature facilitates higher motions of both, molecules constructing MOF scaffold and reaction products. Efficient catalyst turnover and lack of strong H-bond donor or acceptor in

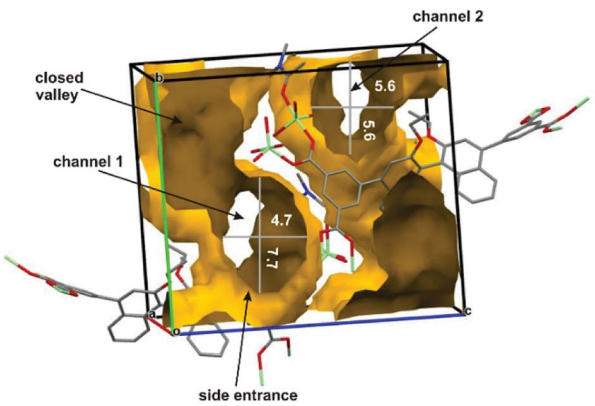

Fig. 2 Connolly's surface calculated from X-ray structure of (*R*)-ZnMOF-**4** showing diameters and topology of two channels.

solid (*R*)-ZnMOF-**4** suggests that probably *N*,*N*-dimethylacetamide molecule coordinated to Zn(II) does not contribute significantly to the stability of the MOF's scaffold and can be replaced by epoxide molecule in catalytic process.

Asymmetric ring-opening reaction

First, we evaluated the catalytic asymmetric ring opening reaction of cyclohexene oxide **5b** with *N*-methylaniline using evacuated (*R*)-CuMOF-**1** as a heterogeneous chiral catalyst. When an equimolar mixture of cyclohexene oxide (0.5 mmol) and *N*-methylaniline (0.5 mmol) was stirred in various solvents (1 mL) in the presence of (*R*)-CuMOF-**1** (10 mol%) at 50 °C for 48 h, optically active β-amino alcohol **6b** was formed in the yields shown in Table 1. Among the various solvents tested, only $CHCl_3$ furnished the desired product **6b** in good yield (86%) with excellent enantioselectivity (85%) (Table 1, entry 2). MeOH, THF or toluene led to almost racemic **6b** in lower yields with poor enantioselectivities (Table 1, entries 1, 3 and 4). The A-B-type stacking mode of (*R*)-CuMOF-**1**[9a] makes it likely that the catalytic reaction takes place on the MOF surface. MeOH and THF solvents interfere the coordination between epoxide and the MOF metal center. On the other hand, toluene molecules might interact with naphthol group through CH–π and π–π interactions and prevent the access of the substrates to the copper-paddlewheel unit affording only the racemic product.

To show the scope of this reaction, we extended it to several cyclic epoxides and *N*-methylanilines using (*R*)-CuMOF-**1** as a catalyst (Table 2). The reaction worked well on five-, six-, and seven-membered epoxides with *N*-methylaniline to form the corresponding β-amino alcohols **6a–6c** with moderate to good enantioselectivities (Table 2, entries 1–3). Of the substituted *N*-methylanilines, *N*-methyl-*p*-toluidine, *N*-methyl-*p*-anisidine and *N*-methyl-*p*-chloroaniline furnished the desired β-amino alcohols **6f–6h** in good yields (85–94%) with excellent enantioselectivities (92–95%) (Table 2, entries 6–8). In contrast, *N*-methyl-*m*-toluidine gave the product **6e** in good yield (90%) but with lower enantioselectivity (78%). The *N*-methyl-*o*-toluidine afforded **6d** in lower efficiency (19% yield) with moderate enantioselectivity (43%), maybe because of the steric constraint (Table 2, entry 4).

Table 1 Effect of solvent on the ARO reactions of cyclohexene oxide and *N*-methyl aniline catalyzed by (*R*)-ZnMOF-**1**

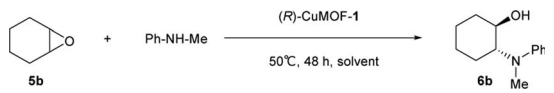

5b **6b**

Entry	Solvent	Yield[a] (%)	Ee[b] (%)	Config.
1	MeOH	23	7	(1*R*,2*R*)
2	$CHCl_3$	86	85	(1*R*,2*R*)
3	THF	1	9	(1*S*,2*S*)
4	Toluene	61	0	(1*R*,2*R*)

[a] Determined by ^{1}H-NMR. [b] HPLC column: Chiralcel OD-H, eluent: hexane/i-PrOH = 98/2, flow rate: 0.3 mL min^{-1}, detection: UV 254 nm.

Table 2 Enantioselective ring-opening reaction of cycloalkane oxide **5** with aromatic amines catalyzed by (*R*)-CuMOF-**1**

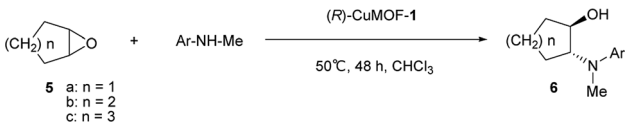

5 a: n = 1, b: n = 2, c: n = 3 **6**

Entry	Epoxide	Ar	Product	Yield (%)	Ee (%)
1	**5a**	Ph	**6a**[d]	93	68[a]
2	**5b**	Ph	**6b**[e]	86	85[a]
3	**5c**	Ph	**6c**	20	89[a]
4	**5b**	2-MePh	**6d**	19	43[a]
5	**5b**	3-MePh	**6e**	90	78[a]
6	**5b**	4-MePh	**6f**	94	92[b]
7	**5b**	4-MeOPh	**6g**	87	95[c]
8	**5b**	4-ClPh	**6h**	85	92[c]

[a] HPLC column: Chiralcel OD-H, eluent: hexane/i-PrOH = 98/2, flow rate: 0.3 mL min^{-1}, detection: UV 254 nm. [b] HPLC column: Chiralcel OB-H, eluent: hexane/i-PrOH = 99/1, flow rate: 0.5 mL min^{-1}, detection: UV 254 nm. [c] HPLC column: Chiralcel OB-H, eluent: hexane/i-PrOH = 95/5, flow rate: 1.0 mL min^{-1}, detection: UV 254 nm. [d] (1*S*,2*S*)-isomer. [e] (1*R*,2*R*)-isomer.

Next, we investigated the aminolysis of *cis*-stilbene oxide with aniline, *N*-methylaniline and 1-naphthylamine by using (*R*)-CuMOF-**1**, (*R*)-CuMOF-**2**, (*R*)-CuMOF-**3** or (*R*)-ZnMOF-**4** as heterogeneous catalysts (Table 3). When an equimolar mixture of *cis*-stilbene oxide and aniline were stirred in various solvents in the presence of evacuated chiral MOFs at several temperatures for 48 h, optically active β-amino alcohols **8a–c** were formed in the yields shown in Table 3. In the presence of (*R*)-CuMOF-**1** as a catalyst, *cis*-stilbene oxide **7** reacted with aniline and *N*-methylaniline at 70 °C for 48 h afforded **8a** and **8b** in 19% and 60% ee, respectively (Table 3, entries 1 and 2). The reaction of *cis*-stilbene oxide **7** with bulky 1-naphthylamine gave **8c** in only 2% yield with 46% ee at 80 °C (Table 3, entry 3).

The reactions of *cis*-stilbene oxide with aniline and *N*-methyl aniline using (*R*)-CuMOF-**2** as a catalyst showed poor reactivity and enantioselectivity (Table 3, entries 4–5), whereas the reaction with bulky 1-naphthylamine furnished the product in 58% yield and with excellent enantioselectivity (97% ee) at 80 °C (Table 3, entry 6). (*R*)-ZnMOF-**4** also exhibited moderate to good enantioselectivities toward the reaction with aniline or *N*-methyl aniline (Table 3, entries 10–11). While (*R*)-ZnMOF-**4** catalyzed reaction with sterically bulky 1-naphthylamine furnished in excellent enantioselectivity of 90% ee at 80 °C (Table 3, entry 12).

In contrast, the ARO reactions catalyzed by (*R*)-CuMOF-**3** afforded the products in lower yields and enantioselectivities (Table 3, entries 7–9).

Then we examined the temperature effect on the ARO reaction of *cis*-stilbene oxide with 1-naphthylamine using (*R*)-CuMOF-**2** as a catalyst (Table 4). As shown in Table 4, the efficient reaction did not occur at temperatures below 50 °C (Table 4, entries 1–4). When the temperature was higher than 60 °C, the ARO reaction occurred efficiently with excellent enantioselectivity up to 97% (Table 4, entries 5–7). A similar temperature

Table 3 Enantioselective ring-opening reaction of *cis*-stilbene oxide with aromatic amines in the presence of several homochiral MOFs

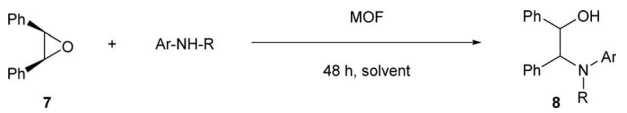

Entry	MOF	Ar	R	Solv.	Product	T (°C)	Yield (%)	Ee[a] (%)
1	(*R*)-**1**	Ph	H	MeOH	**8a**	70	20	19[b]
2	(*R*)-**1**	Ph	Me	MeOH	**8b**	70	38	60[b]
3	(*R*)-**1**	1-Naph	H	2-PrOH	**8c**	80	2	46[c]
4	(*R*)-**2**	Ph	H	2-PrOH	**8a**	80	8	20[c]
5	(*R*)-**2**	Ph	Me	2-PrOH	**8b**	80	11	25[c]
6	(*R*)-**2**	1-Naph	H	2-PrOH	**8c**	80	58	97[c]
7	(*R*)-**3**	Ph	H	2-PrOH	**8a**	80	1	15[c]
8	(*R*)-**3**	Ph	Me	2-PrOH	**8b**	80	19	14[b]
9	(*R*)-**3**	1-Naph	H	2-PrOH	**8c**	80	11	14[b]
10	(*R*)-**4**	Ph	H	2-PrOH	**8a**	80	80	57[b]
11	(*R*)-**4**	Ph	Me	$CHCl_3$	**8b**	50	51	83[b]
12	(*R*)-**4**	1-Naph	H	2-PrOH	**8c**	80	95	90[b]

[a] HPLC column: Chiralcel AD-H, eluent: hexane/i-PrOH = 95/5, flow rate: 1.0 mL min^{-1}, detection: UV 254 nm. [b] (1*S*,2*S*)-isomer. [c] (1*R*,2*R*)-isomer.

effect on the ARO reaction of *cis*-stilbene oxide with anilines has been reported recently.[15]

We also performed control experiments to study the confinement effect of (*R*)-ZnMOF-**4** on the catalyst. When the reaction was performed using $Zn(OAc)_2$ as the catalyst, the product was obtained in 7% yield (Table 5, entry 1). When the reaction was performed using (*R*)-1,1′-bi-2-naphthol (BINOL), the (1*R*,2*R*)-**8c** was obtained in only 4% yield (Table 5, entry 2). When a combination of (*R*)-BINOL and $Zn(OAc)_2$ were used as a catalyst, the reaction proceeded with a similar low efficiency, affording a racemic mixture in 4% yield (Table 5, entry 3). These results clearly showed that the reaction within the framework can develop the enantioselectivity, and this may be attributed to

Table 4 Effect of temperature on the asymmetric ring-opening reaction of *cis*-stilbene oxide with 1-naphthyl amine in the presence of (*R*)-CuMOF-**2** as catalyst

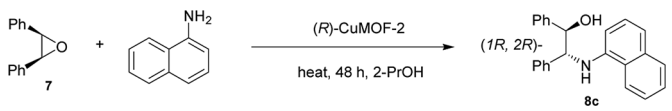

Entry	T (°C)	Yield[a] (%)	Ee[b] (%)
1	20	1	21
2	30	1	32
3	40	2	49
4	50	3	80
5	60	13	95
6	70	22	93
7	80	58	97

[a] Determined by ^{1}H-NMR. [b] Determined by HPLC using Chiralpak AD-H (Daicel).

Table 5 Control experiment of asymmetric ring-opening reactions of *cis*-stilbene oxide and 1-naphthylamine

Entry	Cat.	Yield (%)	Ee[a] (%)	Config.
1	$Zn(OAc)_2$	7	0	—
2	(*R*)-BINOL	Trace	3	(1*R*,2*R*)
3	$Zn(OAc)_2$ + (*R*)-BINOL	4	0	—
4	(*R*)-CuMOF-**1**	4	46	(1*R*,2*R*)
5	(*R*)-CuMOF-**2**	58	97	(1*R*,2*R*)
6	(*R*)-CuMOF-**3**	11	14	(1*S*,2*S*)
7	(*R*)-ZnMOF-**4**	95	90	(1*S*,2*S*)

[a] HPLC column: Chiralcel AD-H, eluent: hexane/i-PrOH = 95/5, flow rate: 1.0 mL min^{-1}, detection: UV 254 nm.

the restricted movement of the substrates in combination with a multiple chiral induction in the confined system. It is also interesting to note that the catalytic activity of (*R*)-ZnMOF-**3**[11] with higher solvent-accessible volume (66% of crystal volume) was lower than that of (*R*)-ZnMOF-**2**[10] (50% of crystal volume) (Table 5, entries 5 and 6).

The reusability of the (*R*)-ZnMOF-**4** catalyst was also investigated for the asymmetric ring-opening reactions of *cis*-stilbene oxide and 1-naphthylamine. As shown in Table 6, (*R*)-ZnMOF-**4** was recovered from the catalytic reaction by filtration, and the recovered catalyst showed a similar high activity in conversion and enantioselectivity. The decreasing reactivity of recovered MOF in 3rd cycle may be due to the loss of the catalyst during the filtration process. To confirm the heterogeneous nature of the reaction, the asymmetric ring-opening reaction of *cis*-stilbene oxide and 1-naphthylamine was performed under the optimized reaction conditions. As shown in Fig. 3, the solid (*R*)-ZnMOF-**4** catalyst was filtered from the reaction mixture after 24 h. The

Table 6 Recycling test of (*R*)-ZnMOF-**4** in asymmetric ring-opening reactions of *cis*-stilbene oxide and 1-naphthylamine

Entry	Cycle	Yield (%)	Ee[a] (%)
1	1st	95	90
2	2nd	91	88
3	3rd	80	91

[a] HPLC column: Chiralcel AD-H, eluent: hexane/i-PrOH = 95/5, flow rate: 1.0 mL min^{-1}, detection: UV 254 nm.

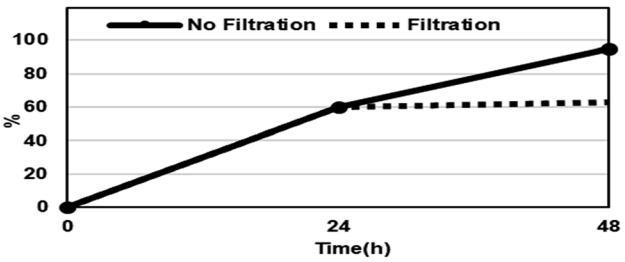

Fig. 3 Heterogeneity test of asymmetric ring-opening reactions of *cis*-stilbene oxide and 1-naphthylamine in the presence of (*R*)-ZnMOF-**4** (straight line) or after filtration of the catalyst at 24 h (dotted line).

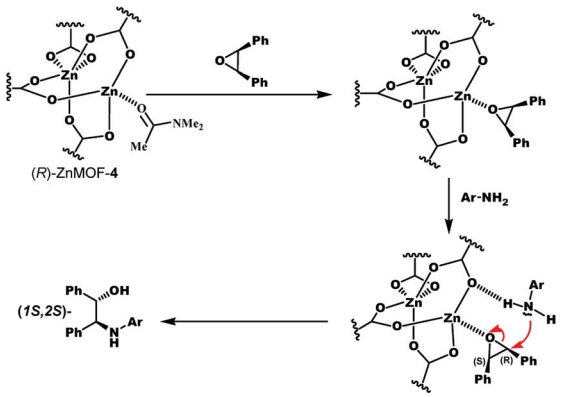

Scheme 1 A plausible mechanism of asymmetric ring-opening reaction of *cis*-stilbene oxide with aromatic amine catalysed by (*R*)-ZnMOF-**4**.

formation of product was interrupted by removing the catalyst from the reaction mixture.

The reaction may proceed as follows: first, *cis*-stilbene oxide coordinates to the Lewis acidic Zn site of (*R*)-ZnMOF-**4** to form an adduct: meanwhile, 1-naphthylamine is fixed by the NH–O hydrogen bond with the carboxylate oxygen and preferentially attacks the adjacent (*R*)-carbon atom of *cis*-stilbene oxide from the backside position to give (1*S*,2*S*)-β-amino alcohol with inversion of stereochemistry (Scheme 1).[9b]

Conclusions

In this work, we have developed an efficient heterogeneous chiral MOF catalyst for the synthesis of β-amino alcohols. The enantioselective ring-opening reaction of cyclohexene oxide with *N*-methylaniline derivatives gave optically active β-amino alcohols in good yields and good to excellent enantioselectivities (up to 95% ee) using (*R*)-CuMOF-**1** as catalyst. On the other hand, (*R*)-CuMOF-**2** and (*R*)-ZnMOF-**4** catalysed ARO reaction of *cis*-stilbene oxide with 1-naphthylamine furnished the corresponding β-amino alcohol in high yield (up to 95%) and excellent enantioselectivity (up to 97% ee). The MOF catalyst was recyclable with retention of the enantioselectivity. Further study of the mechanism and the scope of this reaction are now underway.

Experimental

Synthetic procedures of (*R*)-ZnMOF-4

(*R*)-4,4′-dibromo-2,2′-diethoxy-1,1′-binaphthyl. (*R*)-4,4′-dibromo-2,2′-dihydroxy-1,1′-binaphthyl[12] (100 mg, 0.23 mmol) was dissolved in warm acetone (25 mL). To this was added potassium carbonate (317 mg, 2.3 mmol) and ethyl iodide (0.92 mL, 11.5 mmol) and stirred at room temperature for 24 h. The mixture was then extracted with EtOAc. The organic layers were washed with water and then dried over $MgSO_4$. Removal of the solvent afforded the product as a white solid (110 mg) in 99% yield. Mp: 103–105 °C. ^{1}H NMR ($CDCl_3$, 400 MHz) δ 8.23 (d, J = 8.2 Hz, 1H), 7.73 (s, 1H), 7.45–7.38 (m, 1H), 7.25–7.20 (m, 1H), 7.11 (d, J = 8.2 Hz, 1H), 4.08–3.98 (m, 2H), 1.07 (t, J = 7.1 Hz, 3H). ^{13}C NMR (DMSO-d_6, 100 MHz) δ 154.03, 134.743, 127.90, 127.34, 127.13, 125.82, 125.04, 123.56, 119.96, 119.92, 65.53, 14.99. IR (KCl, cm^{-1}) 3063, 2980, 2925, 1717, 1615, 1578, 1496, 1458, 1413, 1342, 1310, 1259, 1229, 1190, 1101, 1065, 1027, 940, 852, 754, 631, 527, 457, 434, 417.

(*R*)-2,2′-diethoxy-4,4′-di(3,5-bis(methoxycarbonyl)phenyl)-2,2′-binaphthyl. To a degassed mixture of (*R*)-4,4′-dibromo-2,2′-diethoxy-1,1′-binaphthyl (90.2 mg, 0.18 mmol), dimethyl 5-(pinacolboryl)isophthalate (201 mg, 0.63 mmol), and anhydrous K_3PO_4 (382 g, 1.8 mmol) in dry 1,4-dioxane (13 mL) was added $Pd(PPh_3)_4$ (20.8 mg). The resulting mixture was stirred for 72 h at 100 °C under Ar atmosphere. After removal of the solvent, the residue was diluted with $CHCl_3$ and H_2O. The organic phase was separated, and the organic phase was washed with brine and dried over anhydrous $MgSO_4$. After evaporation of the solvent, the residue was purified by flash column chromatography (*n*-hexane–ethyl acetate = 1/1) to give the desired compound as a white solid (94 mg) in 72% yield. Mp: 128–133 °C; ^{1}H NMR ($CDCl_3$, 400 MHz) δ (ppm): 8.83 (t, J = 1.6 Hz, 2H), 8.53 (d, J = 1.4 Hz, 4H), 7.81–7.71 (m, 2H), 7.41 (s, 2H), 7.36–7.20 (m, 6H), 4.21–4.07 (m, 4H), 4.01 (s, 12H), 1.14 (t, J = 6.9 Hz, 6H); ^{13}C NMR (DMSO-d_6, 100 MHz) δ (ppm): 166.36, 153.79, 141.81, 139.37, 135.47, 134.69, 130.92, 129.81, 127.22, 126.49, 126.13, 125.51, 124.22, 120.78, 117.11, 65.40, 52.63, 15.19; IR (KCl, cm^{-1}) 3063, 2980, 2925, 1717, 1615, 1578, 1496, 1458, 1413, 1342, 1310, 1259, 1229, 1190, 1101, 1065, 1027, 940, 852, 754, 631, 527, 457, 434, 417.

(*R*)-2,2′-diethoxy-1,1′-binaphthyl-4,4′-di (5-isophthalic acid) 4. To a methanol solution (1.5 mL) of (*R*)-2,2′-diethoxy-4,4′-di(3,5-bis(methoxycarbonyl)phenyl)-2,2′-binaphthyl (80 mg, 0.11 mmol) was added 6 M NaOH aqueous solution (0.75 mL). The mixture was stirred under reflux for 12 h. Then dil. HCl solution (10 mL) was added to the reaction mixture in an ice-water bath. After removal of the solvent, the residue was diluted with EtOAc and H_2O. The organic phase was separated, and the organic phase was washed with brine and dried over anhydrous $MgSO_4$. After being dried under vacuum, 2,2′-diethoxy-1,1′-binaphthyl-4,4′-di (5-isophthalic acid) was obtained as white solid (67 mg) in 99% yield. Mp: >400 °C. ^{1}H NMR (DMSO-d_6, 400 MHz) δ 13.47 (br, 2H), 8.62 (s, 1H), 8.37 (d, J = 1.8 Hz, 2H), 7.72 (d, J = 7.9 Hz, 1H), 7.61 (s, 1H), 7.38–7.26 (m, 2H), 7.14 (d, J = 7.9 Hz, 1H), 4.26–4.10 (m, 2H), 1.06 (t, J = 7.0 Hz, 3H); ^{13}C NMR (DMSO-d_6, 100 MHz) δ 166.58, 153.42, 140.76, 138.94, 134.63, 134.04, 131.74, 129.15, 126.55, 126.37, 125.55, 125.06, 124.27, 119.51, 116.77, 64.41, 14.86. IR (KCl, cm^{-1}) 2927, 2544, 1701, 1598, 1509, 1447, 1405, 1371, 1340, 1268, 1109, 1064, 1031, 911, 862, 761, 708, 688, 627, 523, 488, 452, 410.

Synthesis of (*R*)-ZnMOF-4

A mixture of (*R*)-2,2′-diethoxy-1,1′-binaphthyl-4,4′-di(5-isophthalic acid) (**4**) (15 mg, 0.02 mmol) and $Cu(NO_3)_2 \cdot 3H_2O$ (15 mg, 0.05 mmol) was dissolved in DMA (2 mL) and EtOH (1 mL). The solution was heated in a screw-capped vial (20 mL) at 110 °C for 48 h to give (*R*)-ZnMOF-**3** (18 mg) as green prisms. IR (KCl, cm^{-1}): 3236, 3067, 2933, 1604, 1508, 1402, 1362, 1265,

1214, 1103, 1029, 918, 862, 816, 769, 715, 593, 475, 457, 419. TGA data for loss of guest solvent: 36%.

General procedure for asymmetric ring-opening reaction

A mixture of *cis*-stilbene oxide (0.042 mmol), aniline derivatives (0.042 mmol) and desolvated (*R*)-ZnMOF-**1** (5 mg) was stirred at indicated temperature and for the indicated time in various solvents (0.3 mL). Then, the solid catalyst was collected by filtration, washed with MeOH, and the solvent of the filtrate were removed in *vacuo* to give the optically active β-amino alcohol. All known compounds were compared with data reported in the literature. The enantiomeric purity and absolute configuration of the product was determined by comparison with the reported HPLC data.[2]

2-(*N*-Methyl-*N*-phenylamino)cyclopentanol

^{1}H-NMR ($CDCl_3$, 400 MHz) δ 7.23–7.19 (m, 2H), 6.86 (d, 2H, J = 8.4 Hz), 6.74–6.71 (m, 1H), 4.18–4.12 (m, 1H), 3.96–3.90 (m, 1H), 2.75 (s, 3H), 2.35 (brs, 1H), 1.96–1.54 (m, 6H). ^{13}C-NMR ($CDCl_3$, 100 MHz) δ 150.97, 128.99, 117.30, 114.16, 74.30, 67.98, 32.13, 31.50, 24.35, 19.82. Enantiomeric excess was determined by HPLC with a Chiralcel OD-H column (Daicel) (*n*-hexane/2-PrOH = 90/10, 1.0 mL min^{-1}, 254 nm).

2-(*N*-Methyl-*N*-phenylamino)cyclohexanol

^{1}H-NMR ($CDCl_3$, 400 MHz) δ 7.25–7.30 (m, 2H), 6.97 (d, 2H, J = 8.6 Hz), 6.83 (t, 1H, J = 8.1 Hz), 3.65–3.71 (ddd, 1H, J = 10.2, 9.9, 4.3 Hz), 3.42–3.46 (m, 1H), 2.80 (bs, 1H), 2.78 (s, 3H), 2.20–2.24 (m, 1H), 1.70–1.80 (m, 3H), 1.27–1.45 (m, 4H). ^{13}C-NMR ($CDCl_3$, 100 MHz) δ 151.32, 129.01, 118.45, 115.52, 69.94, 66.92, 33.29, 31.04, 25.97, 25.40, 24.26. Enantiomeric excess was determined by HPLC with a Chiralcel OD-H column (Daicel) (*n*-hexane/2-PrOH = 98/2, 0.3 mL min^{-1}, 254 nm).

2-(*N*-Methyl-*N*-phenylamino)cycloheptanol

^{1}H-NMR ($CDCl_3$, 400 MHz) δ 7.28–7.24 (m, 2H), 6.96 (d, 2H, J = 7.6 Hz), 6.84 (t, 1H, J = 7.6 Hz), 3.76–3.70 (m, 1H), 3.50–3.44 (m, 1H), 3.08 (brs, 1H), 2.74 (s, 3H), 2.11–2.05 (s, 1H), 1.79–1.37 (m, 9H). ^{13}C-NMR ($CDCl_3$, 100 MHz) δ 151.32, 129.06, 119.01, 116.20, 72.36, 69.49, 32.64, 31.33, 26.67, 25.42, 24.33, 21.72. Enantiomeric excess was determined by HPLC with a Chiralcel OD-H column (Daicel) (eluent: *n*-hexane/2-PrOH = 90 : 10, flow rate: 1.0 mL min^{-1}, 254 nm).

2-(*N*-(2-Methylphenyl)-*N*-methylamino)cyclohexanol

^{1}H-NMR ($CDCl_3$, 400 MHz) δ 7.19–7.11 (m, 3H), 7.02–6.98 (m, 1H), 3.68–3.62 (m, 2H), 2.72–2.66 (m, 4H), 2.35 (s, 3H), 2.18–2.14 (m, 1H), 1.75–1.11 (m, 7H). ^{13}C-NMR ($CDCl_3$, 100 MHz) δ 151.15, 132.98, 131.60, 126.29, 123.61, 122.71, 70.46, 67.86, 33.47, 33.15, 25.38, 24.38, 23.33, 19.09. Enantiomeric excess was determined by HPLC with a Chiralcel OD-H column (Daicel) (*n*-hexane/2-PrOH = 98/2, 0.3 mL min^{-1}, 254 nm).

2-(*N*-(3-Methylphenyl)-*N*-methylamino)cyclohexanol

^{1}H-NMR ($CDCl_3$, 400 MHz) δ 7.14–7.12 (m, 1H), 6.76–6.63 (3, 3H), 3.68–3.62 (m, 1H), 3.42–3.35 (m, 1H), 2.74 (s, 3H), 2.32 (s, 3H), 2.21–2.17 (m, 1H), 1.76–1.67 (m, 4H), 1.42–1.24 (m, 4H). ^{13}C-NMR ($CDCl_3$, 100 MHz) δ 151.44, 138.76, 128.87, 119.46, 116.44, 112.72, 69.95, 67.02, 33.26, 31.07, 25.99, 25.44, 24.30, 21.77. Enantiomeric excess was determined by HPLC with a Chiralcel OD-H column (Daicel) (*n*-hexane/2-PrOH = 98/2, 0.3 mL min^{-1}, 254 nm).

2-(*N*-(4-Methylphenyl)-*N*-methylamino)cyclohexanol

^{1}H-NMR ($CDCl_3$, 400 MHz) δ 7.06 (d, 2H, J = 8.4 Hz), 6.86 (d, 2H, J = 8.8 Hz), 3.66–3.59 (m, 1H), 3.33–3.27 (m, 1H), 2.71 (s, 3H), 2.26 (s, 3H), 2.21–2.16 (m, 1H), 1.77–1.63 (m, 3H). ^{13}C-NMR ($CDCl_3$, 100 MHz) δ 149.20, 129.50, 128.11, 116.22, 69.82, 67.66, 33.23, 31.26, 25.45, 25.43, 24.26, 20.26. Enantiomeric excess was determined by HPLC with a Chiralpak AD-H column (Daicel) (*n*-hexane/2-PrOH = 95/5, 1.0 mL min^{-1}, 254 nm).

2-(*N*-(4-Methoxyphenyl)-*N*-methylamino)cyclohexanol

^{1}H-NMR (CDCl3, 400 MHz) δ 6.93 (d, 2H, J = 9.2 Hz) 6.85 (d, 2H, J = 9.6 Hz), 3.77 (s, 3H), 3.64–3.57 (m, 1H), 3.18–3.12 (m, 2H), 2.69 (s, 3H), 2.21–2.16 (m, 1H), 1.75–1.63 (m, 3H), 1.42–1.19 (m, 4H). ^{13}C-NMR ($CDCl_3$, 100 MHz) δ 153.22, 145.51, 118.59, 114.29, 69.76, 68.94, 55.57, 33.20, 31.91, 25.42, 24.80, 24.25. Enantiomeric excess was determined by HPLC with a Chiralcel OB-H column (Daicel) (*n*-hexane/2-PrOH = 95 : 5, flow rate : 1.0 mL min^{-1}, 254 nm).

2-(*N*-(4-Chlorophenyl)-*N*-methylamino)cyclohexanol

^{1}H-NMR ($CDCl_3$, 400 MHz) δ 7.15 (d, 2H, J = 9.2 Hz), 6.81 (d, 2H, J = 9.2Hz), 3.65–3.58 (m, 1H), 3.44–3.28 (m, 1H), 2.7 (s, 1H), 2.18–2.13 (m, 3H), 1.75–1.63 (m, 3H), 1.42–1.16 (m, 5H). ^{13}C-NMR ($CDCl_3$, 100 MHz) δ 149.89, 128.74, 122.96, 116.40, 69.93, 66.96, 33.34, 31.08, 26.07, 25.31, 24.19. Enantiomeric excess was determined by HPLC with a Chiralcel OB-H column (Daicel) (*n*-hexane/2-PrOH = 95/5, 1.0 mL min^{-1}, 254 nm).

2-Phenylamino-1,2-diphenylethanol

^{1}H-NMR ($CDCl_3$, 400 MHz) δ 7.20–7.09 (m, 10H), 7.04–7.00 (t, J = 8.0 Hz, 2H), 6.62 (t, J = 7.6 Hz, 1H), 6.48 (d, J = 8.0 Hz, 2H), 4.68 (d, J = 6.0 Hz, 1H), 4.42 (d, J = 6.0 Hz, 1H), 2.87 (brs, 1H). ^{13}C-NMR ($CDCl_3$, 100 MHz) δ 147.25, 140.54, 140.22, 129.05, 128.57, 128.26, 127.89, 127.52, 127.26, 126.54, 117.89, 114.11, 78.05, 64.70. Enantiomeric excess was determined by HPLC with a Chiralpak AD-H column (Daicel) (*n*-hexane/2-PrOH = 95/5, 1.0 mL min^{-1}, 254 nm).

2-(*N*-Methyl-*N*-phenylamino)-1,2-diphenylethanol

^{1}H-NMR ($CDCl_3$, 400 MHz) δ 7.37 (d, J = 7.2 Hz, 2H), 7.27–7.07 (m, 8H), 6.99–6.93 (m, 4H), 6.48 (d, J = 8.0 Hz, 2H), 6.90–6.86 (m, 1H), 5.25 (d, J = 10.0 Hz, 1H), 4.86 (d, J = 10.4 Hz, 1H), 4.04 (brs, 1H), 2.64 (s, 3H). ^{13}C-NMR ($CDCl_3$, 100 MHz) δ 151.20, 140.59, 134.60, 129.03, 128.66, 128.11, 127.86, 127.66, 127.55,

127.50, 120.15, 117.53, 73.51, 71.40, 32.56. Enantiomeric excess was determined by HPLC with a Chiralpak AD-H column (Daicel) (*n*-hexane/2-PrOH = 95/5, 1.0 mL min^{-1}, 254 nm).

2-(Naphtalene-1-ylamino)-1,2-diphenylethanol

^{1}H-NMR ($CDCl_3$, 400 MHz) δ 8.01–7.95 (m, 1H), 7.78–7.70 (m, 1H), 7.52–7.42 (m, 2H), 7.39–7.26 (m, 8H), 7.26–7.07 (m, 3H), 6.29 (d, J = 7.3 Hz 1H), 5.55 (s, 1H), 5.05 (d, J = 5.5 Hz, 1H), 4.72 (d, J = 5.5 Hz, 1H), 2.44 (s, 1H). ^{13}C-NMR ($CDCl_3$, 100 MHz) δ 142.11, 140.65, 139.94, 134.19, 128.64, 128.59, 128.34, 127.99, 127.58, 127.19, 126.49, 126.35, 125.64, 124.80, 123.92, 120.00, 117.64, 106.54, 78.28, 64.36. Enantiomeric excess was determined by HPLC with a Chiralpak AD-H column (Daicel) (*n*-hexane/2-PrOH = 95/5, 1.0 mL min^{-1}, 254 nm).

X-ray crystallographic data collection, data processing, structure determination and refinement, thermal analysis, Zn-coordination

A yellow crystal of (*R*)-ZnMOF-**1** of dimensions 0.196 × 0.191 × 0.145 mm was mounted in a cryoloop and transferred to a diffractometer. Intensity data for the single crystal was obtained by collecting reflections on a Bruker X8 diffractometer furnished with an APEX II CCD detector and CuKα (λ = 1.54178 Å) radiation at 296 K using 0.5° ω scans. Integration was done using the SAINT software package[16] that is a part of the APEX II software suite and absorption corrections were conducted using SADABS. Structures were solved *via* direct methods SHELXS-2014.[17] The APEX II program package was used to determine the unit-cell parameters and for data collection (60 sec per frame scan time for a sphere of diffraction data). The raw frame data was processed using SAINT and S4 SADABS to yield the reflection data file. Subsequent calculations were carried out using the SHELXTL program. The diffraction symmetry was consistent with the monoclinic space groups $P2_1$. The structure was solved by direct methods and refined on F^2 by full-matrix least-squares techniques. The analytical scattering factors8 for neutral atoms were used throughout the analysis.

Asymmetric unit contains (*R*)-ZnMOF-**4** ligand, two Zn(II) cations and three *N*,*N*-dimethylacetamide molecules – one coordinated to Zn1 *via* carbonyl O-atom and two other with half occupancy included into the void space of the crystal by CH···O interactions. There were 1.5 molecules of water present in the asymmetric unit – one coordinated to Zn1 atom and the second was distributed over two positions with 0.5 total occupancy. Additionally one ethanol molecule with site occupancy 0.5 is also present in this crystal. Moreover, crystallographic refinement strongly suggests that there are two slightly different ligand molecules present in the studied crystals: one with full ethylation of both hydroxy groups and second, where OH groups was substituted in *ca.* 50% (hard to separate mixture by any of chromatographic methods). Disordered ethyl groups and all solvent molecules were refined in isotropic mode. All non-hydrogen atoms were located *via* difference Fourier maps and refined anisotropically as an inversion twin. Aromatic and methyl/methylene groups hydrogen atom positions were placed at their idealized positions and allowed to ride on the coordinates of the parent atom with isotropic thermal parameters (U_{iso}) fixed at 1.2 U_{eq} of the carbon atom to which they are attached. All solvent molecules were refined in isotropic mode with geometric restraints for all three *N*,*N*-dimethylacetamide molecules. Presence of disorder in the methoxy groups generates close contacts between protons. Refinement converged at wR_2 = 0.1811 refined against 11 706 data (0.80 Å), and R_1 = 0.0664 for 10 606 data with $I > 2.0\sigma(I)$ with GOF = 1.08. There was a single residual density 0.84 e present in the final difference-Fourier map located around Zn atoms (min −0.63 e). crystallographic data have been deposited with the Cambridge Crystallographic Data Centre as CCDC 1832085.

Conflicts of interest

There are no conflicts to declare.

Acknowledgements

This study was supported by a Grant-in-Aid for Scientific Research (C) (No. 26410126) from The Ministry of Education, Culture, Sports, Science and Technology (MEXT). The authors acknowledge the measurement of the BET surface area by the nitrogen adsorption isotherms of (*R*)-ZnMOF-**4** by MicrotracBEL Corp. Osaka, Japan.

Notes and references

1 (*a*) G. A. Rogers, S. M. Parsons, D. C. Anderson, L. M. Nilsson, B. A. Bahr, W. D. Kornreich, R. Kaufman, R. S. Jacobs and B. Kirtman, *J. Med. Chem.*, 1989, **32**, 1217–1230; (*b*) S. C. Bergmeier, *Tetrahedron*, 2000, **56**, 2561–2576.

2 D. J. Ager, I. Prakash and D. R. Schaad, *Chem. Rev.*, 1996, **96**, 835–876.

3 (*a*) E. J. Jacobsen, *Acc. Chem. Res.*, 2000, **33**, 421–431; (*b*) C. Wang, L. Luo and H. Yamamoto, *Acc. Chem. Res.*, 2016, **49**, 193–204; (*c*) S. Meninno and A. Lattanzi, *Chem.–Eur. J.*, 2016, **22**, 3632–3642.

4 (*a*) A. Sekine, T. Ohshima and M. Shibasaki, *Tetrahedron*, 2002, **58**, 75–82; (*b*) G. Bartoli, M. Bosco, A. Carlone, M. Locatelli, M. Massaccesi, P. Melchiorre and L. Sambri, *Org. Lett.*, 2004, **6**, 2173–2176; (*c*) F. Carree, R. Gill and J. Collin, *Org. Lett.*, 2005, **7**, 1023–1026; (*d*) S. Azoulay, K. Manabe and S. Kobayashi, *Org. Lett.*, 2005, **7**, 4593–4595; (*e*) K. Arai, S. Lucarini, M. M. Salter, K. Ohta, Y. Yamashita and S. Kobayashi, *J. Am. Chem. Soc.*, 2007, **129**, 8103–8111; (*f*) E. Mai and C. Schneider, *Chem.–Eur. J.*, 2007, **13**, 2729–2741; (*g*) B. Gao, Y. Wen, Z. Yang, X. Huang, X. Liu and X. Fen, *Adv. Synth. Catal.*, 2008, **350**, 385–390; (*h*) M. Kokubo, T. Naito and S. Kobayashi, *Chem. Lett.*, 2009, **38**, 904–905; (*i*) D. R. Boyd, N. D. Sharma, L. Sbircea, D. Murphy, J. F. Malone, S. L. James, C. C. R. Allen and J. T. G. Hamilton, *Org. Biomol. Chem.*, 2010, **8**, 1081–1090; (*j*) M. Kokubo, T. Naito and S. Kobayashi, *Tetrahedron*, 2010, **66**, 1111–1118; (*k*) R. I. Kureshy, K. J. Prathap, M. Kumar, P. K. Bera, N. H. Khan, S. H. R. Abdi and H. C. Bajaj, *Tetrahedron*, 2011, **67**, 8300–8307; (*l*) B. Gao,

M. Xie, A. Sun, X. Hu, X. Ding, X. Liu, L. Lin and X. Feng, *Adv. Synth. Catal.*, 2012, **354**, 1509–1518; (*m*) G. V. More and B. M. Bhanage, *Eur. J. Org. Chem.*, 2013, 6900–6906; (*n*) M. Kumar, R. I. Kureshy, S. Saravanan, S. Verma, A. Jakhar, N. H. Khan, S. H. R. Abdi and H. C. Baja, *Org. Lett.*, 2014, **16**, 2798–2801; (*o*) A. Sharma, J. Agarwal and R. K. Peddinti, *Org. Biomol. Chem.*, 2017, **15**, 1913–1920.

5 (*a*) A. Phan, C. J. Doonan, F. J. Uribe-Romo, C. B. Knobler, M. O'Keeffe and O. M. Yaghi, *Acc. Chem. Res.*, 2010, **43**, 58–67; (*b*) K. Sumida, D. L. Rogow, J. A. Mason, T. M. McDonald, E. D. Bloch, Z. R. Herm, T. Bae and J. R. Long, *Chem. Rev.*, 2012, **112**, 724–781; (*c*) B. Van de Voorde, B. Bueken, J. Denayer and D. De Vos, *Chem. Soc. Rev.*, 2014, **43**, 5766–5788; (*d*) I. Cota and M. F. Fernandez, *Coord. Chem. Rev.*, 2017, **351**, 189–204.

6 (*a*) P. Peluso, V. Mamane and S. Cossu, *J. Chromatogr. A*, 2014, **1363**, 11–26; (*b*) D. Banerjee, A. J. Cairns, J. Liu, R. K. Motkuri, S. K. Nune, C. A. Fernandez, R. Krishna, D. M. Strachan and P. K. Thallapally, *Acc. Chem. Res.*, 2015, **48**, 211–219; (*c*) L. Heinke, M. Tu, S. Wannapaiboon, R. Fischer and C. Woell, *Microporous Mesoporous Mater.*, 2015, **216**, 200–215.

7 (*a*) L. E. Kreno, K. Leong, O. K. Farha, M. Allendorf, R. P. Van Duyne and J. T. Hupp, *Chem. Rev.*, 2012, **112**, 1105–1125; (*b*) D. Liu, K. Lu, C. Poon and W. Lin, *Inorg. Chem.*, 2014, **53**, 1916–1924; (*c*) A. Karmakar, P. Samanta, A. V. Desai and S. K. Ghosh, *Acc. Chem. Res.*, 2017, **50**, 2457–2469.

8 (*a*) L. Ma, C. Abney and W. Lin, *Chem. Soc. Rev.*, 2009, **38**, 1248–1256; (*b*) J. Y. Lee, O. K. Farha, J. Roberts, K. A. Scheidt, B. T. Nguyen and J. T. Hupp, *Chem. Soc. Rev.*, 2009, **38**, 1450–1459; (*c*) L. Ma and W. Lin, *Top. Curr. Chem.*, 2010, **293**, 175–205; (*d*) J. Liu, L. Chen, H. Cui, J. Zhang, L. Zhang and C. Su, *Chem. Soc. Rev.*, 2014, **43**, 6011–6061; (*e*) A. H. Chughtai, N. Ahmad, H. A. Younus, A. Laypkov and F. Verpoort, *Chem. Soc. Rev.*, 2015, **44**, 6804–6849; (*f*) Y. Zhang, J. Guo, L. Shi, Y. Zhu, K. Hou, Y. Zheng and Z. Tang, *Sci. Adv.*, 2017, **3**, e1701162; (*g*) W. Shi, L. Cao, H. Zhang, X. Zhou, B. An, Z. Lin, R. Dai, J. Li, C. Wang and W. Lin, *Angew. Chem., Int. Ed.*, 2017, **56**, 9704–9709.

9 (*a*) K. Tanaka, S. Oda and M. Shiro, *Chem. Commun.*, 2008, 820–822; (*b*) K. Doitomi, K. Xua and H. Hirao, *Dalton Trans.*, 2017, **46**, 3470–3481.

10 K. Tanaka, S. Nagase, T. Anami, M. Wierzbickib and Z. Urbanczyk-Lipkowska, *RSC Adv.*, 2016, **6**, 111436–111439.

11 K. Tanaka, D. Yanamoto, K. Yoshimura, T. Anamia and Z. Urbanczyk-Lipkowska, *CrystEngComm*, 2015, **17**, 1291–1295.

12 M. W. A. MacLean, T. K. Wood, G. Wu, R. P. Lemieux and C. M. Crudden, *Chem. Mater.*, 2014, **26**, 5852–5859.

13 M. L. Connolly, *Science*, 1983, **221**, 709.

14 R. I. Kureshy, S. Singh, N. H. Khana, S. H. R. Abdi, E. Suresh and R. V. Jasra, *J. Mol. Catal. A: Chem.*, 2007, **264**, 162–169.

15 S. Regati, Y. He, M. Thimmaiah, R. Li, S. Xiang, B. Chen and J. C. G. Zhao, *Chem. Commun.*, 2013, **49**, 9836–9838.

16 Bruker, *APEX2*, SAINT and SADABS Bruker AXS Inc., Madison, Wisconsin, USA, 2005.

17 G. M. Sheldrick, Program for the Refinement of Crystal Structures from Diffraction Data, *SHELXL-2014*, University of Göttingen, Germany, 2014.